

---

# Universal approximation and model compression for radial neural networks

---

Anonymous Author(s)

Affiliation

Address

email

## Abstract

1 We introduce a class of fully-connected neural networks whose activa-  
2 tion functions, rather than being pointwise, rescale feature vectors by a  
3 function depending only on their norm. We call such networks *radial*  
4 neural networks, extending previous work on rotation equivariant net-  
5 works that considers rescaling activations in less generality. We prove  
6 universal approximation theorems for radial neural networks, including  
7 in the more difficult cases of bounded widths and unbounded domains.  
8 Our proof techniques are novel, distinct from those in the pointwise case.  
9 Additionally, radial neural networks exhibit a rich group of orthogonal  
10 change-of-basis symmetries on the vector space of trainable parameters.  
11 Factoring out these symmetries leads to a practical lossless model com-  
12 pression algorithm. Optimization of the compressed model by gradient  
13 descent is equivalent to projected gradient descent for the full model.

## 14 1 Introduction

15 Inspired by biological neural networks, the theory of artificial neural networks has largely  
16 focused on pointwise (or “local”) nonlinear layers [46, 14], in which the same function  
17  $\sigma: \mathbb{R} \rightarrow \mathbb{R}$  is applied to each coordinate independently:

$$\mathbb{R}^n \rightarrow \mathbb{R}^n, \quad v = (v_1, \dots, v_n) \mapsto (\sigma(v_1), \sigma(v_2), \dots, \sigma(v_n)). \quad (1.1)$$

18 In networks with pointwise nonlinearities, the standard basis vectors in  $\mathbb{R}^n$  can be inter-  
19 preted as “neurons” and the nonlinearity as a “neuron activation.” Research has generally  
20 focused on finding functions  $\sigma$  which lead to more stable training, have less sensitivity to  
21 initialization, or are better adapted to certain applications [42, 38, 37, 10, 29]. Many  $\sigma$  have  
22 been considered, including sigmoid, ReLU, arctangent, ELU, Swish, and others.

23 However, by setting aside the biological metaphor, it is possible to consider a much  
24 broader class of nonlinearities, which are not necessarily pointwise, but instead depend  
25 simultaneously on many coordinates. Neural networks using such nonlinearities may yield  
26 expressive function classes with different advantages. One example is radial basis networks  
27 [4], which contain nonlinearities of the form  $\|v - c\|$ , which depend on all coordinates of  $v$ .  
28 However, each coordinate output is still independent.

29 In this paper, we introduce *radial* neural networks which employ non-pointwise nonlin-  
30 earities called *radial rescaling* activations. Freedom from the pointwise assumption allows  
31 us to design activation functions that maximize symmetry in the parameter space of the

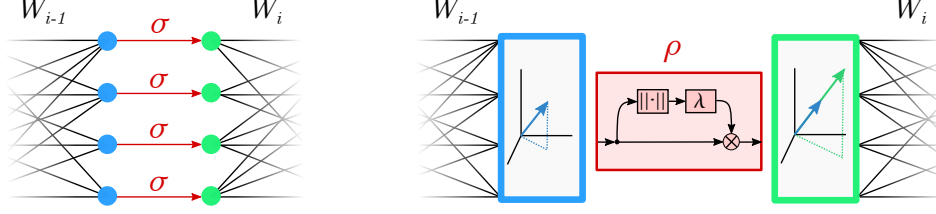


Figure 1: (Left) Pointwise activations distinguish a specific basis of each hidden layer and treat each coordinate independently, see equation 1.1. (Right) Radial rescaling activations rescale each feature vector by a function of the norm, see equation 1.2.

neural network. Such networks enjoy several provable properties including high model compressibility, symmetry in optimization, and universal approximation. These activations are defined by rescaling each vector by a scalar that depends only on the norm of the vector:

$$\rho : \mathbb{R}^n \rightarrow \mathbb{R}^n, \quad v \mapsto \lambda(|v|)v, \quad (1.2)$$

where  $\lambda$  is a scalar-valued function of the norm. Whereas in the pointwise setting, only the linear layers mix information between different components of the latent features, for radial rescaling, all coordinates of the activation output vector are affected by all coordinates of the activation input vector. The inherent geometric symmetry of radial rescalings makes them particularly useful for designing equivariant neural networks [55, 47, 56, 57].

In our first set of main results, we prove that radial neural networks are in fact *universal approximators*. Specifically, we demonstrate that any asymptotically affine function can be approximated with a radial neural network, suggesting potentially good extrapolation behavior. Moreover, this approximation can be done with bounded width. Our approach to proving these results differs significantly from standard techniques used in the case of pointwise activations due to the fact that coordinates cannot be treated independently when dealing with non-pointwise activations.

In our second set of main results, we exploit parameter space symmetries of radial neural networks to achieve *model compression*. Using the fact that radial rescaling activations commute with orthogonal transformations, we develop a practical algorithm to systematically factor out orthogonal symmetries via iterated QR decompositions. This leads to another radial neural network with fewer neurons in each hidden layer. The resulting model compression algorithm is *lossless*: the compressed network and the original network both have the same value of the loss function on any batch of training data.

Furthermore, we prove that the loss of the compressed model after one step of gradient descent is equal to the loss of the original model after one step of *projected gradient descent*. As explained below, projected gradient descent involves zeroing out certain parameter values after each step of gradient descent. Although training the original network may result in a lower loss function after fewer epochs, in many cases the compressed network takes less time per epoch to train and is faster in reaching a local minimum.

To summarize, our main contributions are:

- A formalization of radial neural networks, a new class of neural networks;
- Two universal approximations results for radial neural networks: a) approximation of asymptotically affine functions, and b) bounded width approximation;
- An implementation of a lossless model compression algorithm for radial neural networks;
- A theorem providing the precise relationship between gradient descent optimization of the original and compressed networks.

## 69 2 Related work

70 **Radial rescaling activations.** Radial rescaling functions have the symmetry property  
 71 of preserving vector directions, and hence exhibit rotation equivariance. Consequently,  
 72 examples of such functions, such as the squashing nonlinearity and Norm-ReLU, feature in  
 73 the study of rotationally equivariant neural networks [55, 47, 56, 57, 26]. However, previous  
 74 works apply the activation only along the channel dimension, and consider the orthogonal  
 75 group  $O(n)$  only for  $n = 2, 3$ . In contrast, we consider a radial rescaling activation across  
 76 the entire hidden layer, and  $O(n)$ -equivariance where  $n$  is the hidden layer dimension. Our  
 77 constructions echo the vector neurons formalism [15], in which the output of a nonlinearity  
 78 is a vector rather than a scalar. For radial basis networks, each hidden neuron is a radial  
 79 nonlinear function of the shifted input vector, but the outputs are independent, whereas  
 80 for radial rescaling functions, the outputs are also tied together [4].

81 **Universal approximation.** Neural networks of arbitrary width and sigmoid activations  
 82 have long been known to be universal approximators [14]. Universal approximation can  
 83 also be achieved by bounded width networks with arbitrary depth [36]. Additional work  
 84 has generalized to other activation functions and neural architectures [24, 60, 43, 50]. While  
 85 most work has focused on compact domains, some recent work also considers non-compact  
 86 domains [28, 54]. The techniques used for pointwise activation functions generalize to  
 87 radial basis networks since the outputs of each RBF are independent [40], but do not easily  
 88 generalize to the radial rescaling activations considered here, because all coordinates of the  
 89 activation output vector are affected by all coordinates of the activation input vector. As a  
 90 consequence, individual radial neural network approximators of two different functions  
 91 cannot be easily combined to give an approximator of the sum of the functions.

92 **Groups and symmetry.** Appearances of symmetry in machine learning have generally  
 93 focused on symmetric input and output spaces. Most prominently, equivariant neural  
 94 networks incorporate symmetry as an inductive bias and feature weight-sharing constraints  
 95 based on equivariance with respect to various symmetry groups. Examples of equivariant  
 96 architectures include G-convolution, steerable CNN, and Clebsch-Gordon networks [13, 55,  
 97 11, 9, 30, 2, 58, 12, 57, 16, 31, 44]. By contrast, our approach to radial neural networks does  
 98 not depend on symmetries of the input domain, output space, or feedforward mapping.  
 99 Instead, we exploit parameter space symmetries and thus obtain more general results that  
 100 apply to domains with no apparent symmetry.

101 **Model compression.** A major goal in machine learning is to find methods to reduce  
 102 the number of trainable parameters, decrease memory usage, or accelerate inference and  
 103 training [8, 61]. Our approach toward this goal differs significantly from most existing  
 104 methods in that it is based on the inherent symmetry of network parameter spaces. One  
 105 prior method is *weight pruning*, which removes redundant or small weights from a network  
 106 with little loss in accuracy [20, 3, 27]. Pruning can be done during training [18] or at  
 107 initialization [34, 53]. *Gradient-based pruning* identifies low saliency weights by estimating  
 108 the increase in loss resulting from their removal [33, 22, 17, 39]. A complementary approach  
 109 is *quantization*, which decreases the bit depth of weights [59, 25, 19]. *Knowledge distillation*  
 110 identifies a small model mimicking the performance of a larger model or ensemble  
 111 of models [5, 23, 1]. *Matrix Factorization* methods replace fully connected layers with  
 112 lower rank or sparse factored tensors [6, 7, 52, 32, 45, 35] and can often be applied  
 113 before training. Our method involves a type of matrix factorization based on the QR  
 114 decomposition; however, rather than aim for a rank reduction of linear layers, we leverage  
 115 this decomposition to reduce hidden widths via change-of-basis operations on the hidden  
 116 representations. Close to our method are lossless compression methods which remove  
 117 stable neurons in ReLU networks [49, 48] or exploit permutation parameter space symmetry  
 118 to remove redundant neurons [51]; our compression instead follows from the symmetries  
 119 of the radial rescaling activation. Finally, the model compression results of [26], while  
 120 conceptually similar to ours, are weaker, as (1) the unitary group action is on disjoint layers  
 121 instead of iteratively moving through all layers, and (2) the results are only stated for a  
 122 version of the squashing nonlinearity.

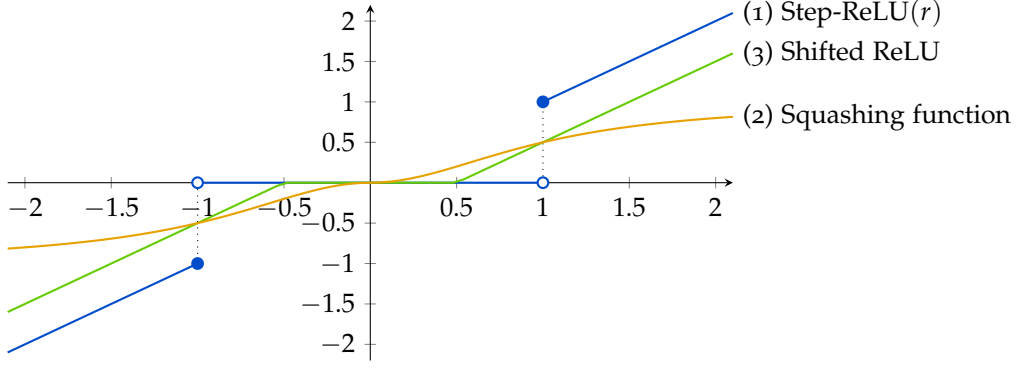


Figure 2: Examples of different radial rescaling functions in  $\mathbb{R}^1$ , see [Example 1](#).

### 123 3 Radial neural networks

124 In this section, we define radial rescaling functions and radial neural networks. Let  
 125  $h : \mathbb{R} \rightarrow \mathbb{R}$  be a function. For any  $n \geq 1$ , set:

$$h^{(n)} : \mathbb{R}^n \rightarrow \mathbb{R}^n \quad h^{(n)}(v) = h(|v|) \frac{v}{|v|}$$

126 for  $v \neq 0$ , and  $h^{(n)}(0) = 0$ . A function  $\rho : \mathbb{R}^n \rightarrow \mathbb{R}^n$  is called a *radial rescaling* function if  
 127  $\rho = h^{(n)}$  for some piecewise differentiable  $h : \mathbb{R} \rightarrow \mathbb{R}$ . Hence,  $\rho$  sends each input vector to  
 128 a scalar multiple of itself, and that scalar depends only on the norm of the vector<sup>1</sup>. It is  
 129 easy to show that radial rescaling functions commute with orthogonal transformations.

130 **Example 1.** (1) Step-ReLU, where  $h(r) = r$  if  $r \geq 1$  and 0 otherwise. In this case, the radial  
 131 rescaling function is given by

$$\rho : \mathbb{R}^n \rightarrow \mathbb{R}^n, \quad v \mapsto v \text{ if } |v| \geq 1; \quad v \mapsto 0 \text{ if } |v| < 1 \quad (3.1)$$

132 (2) The squashing function, where  $h(r) = r^2/(r^2 + 1)$ . (3) Shifted ReLU, where  $h(r) =$   
 133  $\max(0, r - b)$  for  $r > 0$  and  $b$  is a real number. See Figure 2. We refer to [55] and the  
 134 references therein for more examples and discussion of radial functions.

135 A *radial neural network* with  $L$  layers consists of a positive integer  $n_i$  indicating the width of  
 136 each layer  $i = 0, 1, \dots, L$ ; the trainable parameters, comprising of a matrix  $W_i \in \mathbb{R}^{n_i \times n_{i-1}}$   
 137 of weights and a bias vector  $b_i \in \mathbb{R}^{n_i}$  for each  $i = 1, \dots, L$ ; and a radial rescaling function  
 138  $\rho_i : \mathbb{R}^{n_i} \rightarrow \mathbb{R}^{n_i}$  for each  $i = 1, \dots, L$ . We refer to the tuple  $\mathbf{n} = (n_0, n_1, \dots, n_L)$  as the *widths*  
 139 *vector* of the neural network. The hidden widths vector is  $\mathbf{n}^{\text{hid}} = (n_1, n_2, \dots, n_{L-1})$ . The  
 140 feedforward function  $F : \mathbb{R}^{n_0} \rightarrow \mathbb{R}^{n_L}$  of a radial neural network is defined in the usual way  
 141 as an iterated composition of affine maps and activations. Explicitly, set  $F_0 = \text{id}_{\mathbb{R}^{n_0}}$  and  
 142 recursively define the partial feedforward functions:

$$F_i : \mathbb{R}^{n_0} \rightarrow \mathbb{R}^{n_i}, \quad x \mapsto \rho_i(W_i \circ F_{i-1}(x) + b_i)$$

143 for  $i = 1, \dots, L$ . Then the feedforward function is  $F = F_L$ .

144 **Remark 2.** If  $b_i = 0$  for all  $i$ , then the feedforward function takes the form  $F(x) = W(\mu(x)x)$   
 145 where  $\mu : \mathbb{R}^n \rightarrow \mathbb{R}$  is a scalar-valued function and  $W = W_L W_{L-1} \cdots W_1 \in \mathbb{R}^{n_L \times n_0}$  is the  
 146 product of the weight matrices. If any of the biases are non-zero, then the feedforward  
 147 function lacks such a simple form.

<sup>1</sup>A function  $\mathbb{R}^n \rightarrow \mathbb{R}$  that depends only on the norm of a vector is known as a *radial* function. Radial rescaling functions rescale each vector according to the radial function  $v \mapsto \lambda(|v|) = \frac{h(|v|)}{|v|}$ . This explains the connection to Equation 1.2.

## 148 4 Universal Approximation

149 In this section, we consider two universal approximation results. The first approxi-  
 150 mates asymptotically affine functions with a network of unbounded width. The second  
 151 generalizes to bounded width networks. Proofs appear in Appendix B. Throughout,  
 152  $B_r(c) = \{x \in \mathbb{R}^n : |x - c| < r\}$  denotes the  $r$ -ball around a point  $c$ , and an affine map  
 153  $\mathbb{R}^n \rightarrow \mathbb{R}^m$  is one of the form  $L(x) = Ax + b$  for a matrix  $A \in \mathbb{R}^{m \times n}$  and  $b \in \mathbb{R}^m$ .

### 154 4.1 Approximation of asymptotically affine functions

155 A continuous function  $f : \mathbb{R}^n \rightarrow \mathbb{R}^m$  is said to be *asymptotically affine* if there exists an  
 156 affine map  $L : \mathbb{R}^n \rightarrow \mathbb{R}^m$  such that, for every  $\epsilon > 0$ , there is a compact subset  $K$  of  $\mathbb{R}^n$   
 157 such that  $|L(x) - f(x)| < \epsilon$  for all  $x \in \mathbb{R}^n \setminus K$ . In particular, continuous functions with  
 158 compact support are asymptotically affine. The continuity of  $f$  and compactness of  $K$  imply  
 159 that, for any  $\epsilon > 0$ , there exist  $c_1, \dots, c_N \in K$  and  $r_1, \dots, r_N \in (0, 1)$  such that, first, the  
 160 union of the balls  $B_{r_i}(c_i)$  covers  $K$  and, second, for all  $i$ , we have  $f(B_{r_i}(c_i) \cap K) \subseteq B_\epsilon(f(c_i))$ .  
 161 Let  $N(f, K, \epsilon)$  be the minimal choice of  $N$ . In many cases, the constant  $N(f, K, \epsilon)$  can be  
 162 bounded explicitly<sup>2</sup>.

163 **Theorem 3** (Universal approximation). *Let  $f : \mathbb{R}^n \rightarrow \mathbb{R}^m$  be an asymptotically affine function.*  
 164 *For any  $\epsilon > 0$ , there exists a compact set  $K \subset \mathbb{R}^n$  and a function  $F : \mathbb{R}^n \rightarrow \mathbb{R}^m$  such that:*

- 165 1.  *$F$  is the feedforward function of a radial neural network with  $N = N(f, K, \epsilon)$  layers whose*  
 166 *hidden widths are  $(n + 1, n + 2, \dots, n + N)$ .*
- 167 2. *For any  $x \in \mathbb{R}^n$ , we have  $|F(x) - f(x)| < \epsilon$ .*

168 We note that the approximation in Theorem 3 is valid on all of  $\mathbb{R}^n$ . To give an idea of the  
 169 proof, first fix  $c_1, \dots, c_N \in K$  and  $r_1, \dots, r_N \in (0, 1)$  as above. Let  $e_1, \dots, e_N$  be orthonormal  
 170 basis vectors extending  $\mathbb{R}^n$  to  $\mathbb{R}^{n+N}$ . For  $i = 1, \dots, N$  define the following affine maps:

$$\begin{aligned} T_i : \mathbb{R}^{n+i-1} &\rightarrow \mathbb{R}^{n+i} & S_i : \mathbb{R}^{n+i} &\rightarrow \mathbb{R}^{n+i} \\ z &\mapsto z - c_i + h_i e_i & z &\mapsto z - (1 + h_i^{-1}) \langle e_i, z \rangle e_i + c_i + e_i \end{aligned}$$

171 where  $h_i = \sqrt{1 - r_i^2}$  and  $\langle e_i, z \rangle$  is the coefficient of  $e_i$  in  $z$ . Setting  $\rho_i$  to be Step-ReLU  
 172 (Equation 3.1) on  $\mathbb{R}^{n+i}$ , these maps are chosen so that the composition  $S_i \circ \rho_i \circ T_i$  maps  
 173 the points in  $B_{r_i}(c_i)$  to  $c_i + e_i$ , while keeping points outside this ball the same. We now  
 174 describe a radial neural network with widths  $(n, n + 1, \dots, n + N, m)$  whose feedforward  
 175 function approximates  $f$ . For  $i = 1, \dots, N$  the affine map from layer  $i - 1$  to layer  $i$  is given  
 176 by  $z \mapsto T_i \circ S_{i-1}(z)$ , with  $S_0 = \text{id}_{\mathbb{R}^n}$ . The activation at each hidden layer is Step-ReLU. Let  
 177  $L$  be the affine map such that  $|L - f| < \epsilon$  on  $\mathbb{R}^n \setminus K$ . The affine map from layer  $N$  to the  
 178 output layer is  $\Phi \circ S_N$  where  $\Phi : \mathbb{R}^{n+N} \rightarrow \mathbb{R}^m$  is the unique affine map determined by  
 179  $x \mapsto L(x)$  if  $x \in \mathbb{R}^n$ , and  $e_i \mapsto f(c_i) - L(c_i)$ . This construction is illustrated in Figure 3.

### 180 4.2 Bounded width approximation

181 We now turn our attention to a bounded width universal approximation result.

182 **Theorem 4.** *Let  $f : \mathbb{R}^n \rightarrow \mathbb{R}^m$  be an asymptotically affine function. For any  $\epsilon > 0$ , there exists a*  
 183 *compact set  $K \subset \mathbb{R}^n$  and a function  $F : \mathbb{R}^n \rightarrow \mathbb{R}^m$  such that:*

- 184 1.  *$F$  is the feedforward function of a radial neural network with  $N = N(f, K, \epsilon)$  hidden*  
 185 *layers whose widths are all  $n + m + 1$ .*
- 186 2. *For any  $x \in \mathbb{R}^n$ , we have  $|F(x) - f(x)| < \epsilon$ .*

187 The proof, which is more involved than that of Theorem 3, relies on using orthogonal  
 188 dimensions to represent the domain and the range of  $f$ , together with an indicator

<sup>2</sup>For example, if  $K$  is the unit cube in  $\mathbb{R}^n$  and  $f$  is Lipschitz continuous with Lipschitz constant  $R$ ,  
 then  $N(f, K, \epsilon) \leq \left\lceil \frac{R\sqrt{n}}{2\epsilon} \right\rceil^n$ .

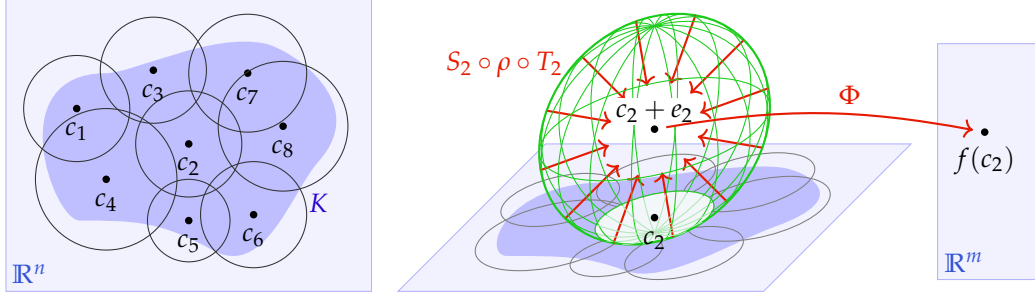


Figure 3: Two layers of the radial neural network used in the proof of Theorem 3. (Left) The compact set  $K$  is covered with open balls. (Middle) Points close to  $c_2$  (green ball) are mapped to  $c_2 + e_2$ , all other points are kept the same. (Right) In the final layer,  $c_2 + e_2$  is mapped to  $f(c_2)$ .

dimension to distinguish the two. We regard points in  $\mathbb{R}^{n+m+1}$  as triples  $(x, y, \theta)$  where  $x \in \mathbb{R}^n, y \in \mathbb{R}^m$  and  $\theta \in \mathbb{R}$ . The proof of Theorem 4 parallels that of Theorem 3, but instead of mapping points in  $B_{r_i}(c_i)$  to  $c_i + e_i$ , we map the points in  $B_{r_i}((c_i, 0, 0))$  to  $(0, \frac{f(c_i) - L(0)}{s}, 1)$ , where  $s$  is chosen such that different balls do not interfere. The final layer then uses an affine map  $(x, y, \theta) \mapsto L(x) + sy$ , which takes  $(x, 0, 0)$  to  $L(x)$ , and  $(0, \frac{f(c_i) - L(0)}{s}, 1)$  to  $f(c_i)$ . We remark on several additional results; see Appendix B for full statements and proofs. The bound of Theorem 4 can be strengthened to  $\max(n, m) + 1$  in the case of functions  $f : K \rightarrow \mathbb{R}^m$  defined on a compact domain  $K \subset \mathbb{R}^n$  (i.e., ignoring asymptotic behavior). Furthermore, with more layers, it is possible to reduce that bound to  $\max(n, m)$ .

## 5 Model compression

In this section, we prove a model compression result. Specifically, we provide an algorithm which, given any radial neural network, computes a different radial neural network with smaller widths. The resulting compressed network has the same feedforward function as the original network, and hence the same value of the loss function on any batch of training data. In other words, our model compression procedure is *lossless*. Although our algorithm is practical and explicit, it reflects more conceptual phenomena, namely, a change-of-basis action on network parameter spaces (Section 5.1).

### 5.1 The parameter space

Suppose a fully connected network has  $L$  layers and widths given by the tuple  $\mathbf{n} = (n_0, n_1, n_2, \dots, n_{L-1}, n_L)$ . In other words, the  $i$ -th layer has input width  $n_{i-1}$  and output width  $n_i$ . The parameter space is defined as the vector space of all possible choices of parameter values. Hence, it is given by the following product of vector spaces:

$$\text{Param}(\mathbf{n}) = (\mathbb{R}^{n_1 \times n_0} \times \mathbb{R}^{n_2 \times n_1} \times \dots \times \mathbb{R}^{n_L \times n_{L-1}}) \times (\mathbb{R}^{n_1} \times \mathbb{R}^{n_2} \times \dots \times \mathbb{R}^{n_L})$$

We denote an element therein as a pair of tuples  $(\mathbf{W}, \mathbf{b})$  where  $\mathbf{W} = (W_i \in \mathbb{R}^{n_i \times n_{i-1}})_{i=1}^L$  are the weights and  $\mathbf{b} = (b_i \in \mathbb{R}^{n_i})_{i=1}^L$  are the biases. To describe certain symmetries of the parameter space, consider the following product of orthogonal groups, with sizes corresponding to the widths of the hidden layers:

$$O(\mathbf{n}^{\text{hid}}) = O(n_1) \times O(n_2) \times \dots \times O(n_{L-1})$$

There is a change-of-basis action of  $O(\mathbf{n}^{\text{hid}})$  on the parameter space  $\text{Param}(\mathbf{n})$ . Explicitly, the tuple of orthogonal matrices  $\mathbf{Q} = (Q_i)_{i=1}^{L-1} \in O(\mathbf{n}^{\text{hid}})$  transforms the parameter values

$(\mathbf{W}, \mathbf{b})$  to  $\mathbf{Q} \cdot \mathbf{W} := (Q_i W_i Q_{i-1}^{-1})_{i=1}^L$  and  $\mathbf{Q} \cdot \mathbf{b} := (Q_i b_i)_{i=1}^L$ , where  $Q_0 = \text{id}_{n_0}$  and  $Q_L = \text{id}_{n_L}$ .

We write  $\mathbf{Q} \cdot (\mathbf{W}, \mathbf{b})$  for  $(\mathbf{Q} \cdot \mathbf{W}, \mathbf{Q} \cdot \mathbf{b})$ .



## 219 5.2 Model compression

220 In order to state the compression result, we first define the reduced widths. Namely,  
 221 the reduction  $\mathbf{n}^{\text{red}} = (n_0^{\text{red}}, n_1^{\text{red}}, \dots, n_L^{\text{red}})$  of a widths vector  $\mathbf{n}$  is defined recursively by  
 222 setting  $n_0^{\text{red}} = n_0$ , then  $n_i^{\text{red}} = \min(n_i, n_{i-1}^{\text{red}} + 1)$  for  $i = 1, \dots, L-1$ , and finally  $n_L^{\text{red}} =$   
 223  $n_L$ . For a tuple  $\rho = (\rho_i : \mathbb{R}^{n_i} \rightarrow \mathbb{R}^{n_i})_{i=1}^L$  of radial rescaling functions, we write  $\rho^{\text{red}} =$   
 224  $(\rho_i^{\text{red}} : \mathbb{R}^{n_i^{\text{red}}} \rightarrow \mathbb{R}^{n_i^{\text{red}}})$  for the corresponding tuple of restrictions, which are all radial  
 225 rescaling functions. The following result relies on Algorithm 1 below.

226 **Theorem 5.** Let  $(\mathbf{W}, \mathbf{b}, \rho)$  be a radial neural network with widths  $\mathbf{n}$ . Let  $\mathbf{W}^{\text{red}}$  and  $\mathbf{b}^{\text{red}}$  be the  
 227 weights and biases of the compressed network produced by Algorithm 1. The feedforward function  
 228 of the original network  $(\mathbf{W}, \mathbf{b}, \rho)$  coincides with that of the compressed network  $(\mathbf{W}^{\text{red}}, \mathbf{b}^{\text{red}}, \rho^{\text{red}})$ .

---

### Algorithm 1: QR Model Compression (QR-compress)

---

```

input   :  $\mathbf{W}, \mathbf{b} \in \text{Param}(\mathbf{n})$ 
output  :  $\mathbf{Q} \in O(\mathbf{n}^{\text{hid}})$  and  $\mathbf{W}^{\text{red}}, \mathbf{b}^{\text{red}} \in \text{Param}(\mathbf{n}^{\text{red}})$ 

 $\mathbf{Q}, \mathbf{W}^{\text{red}}, \mathbf{b}^{\text{red}} \leftarrow [], [], []$                                 // initialize output lists
 $A_1 \leftarrow [b_1 \quad W_1]$                                        // matrix of size  $n_1 \times (n_0 + 1)$ 
for  $i \leftarrow 1$  to  $L-1$  do                                       // iterate through layers
     $Q_i, R_i \leftarrow \text{QR-decomp}(A_i, \text{mode} = \text{'complete'})$       //  $A_i = Q_i \text{Inc}_i R_i$ 
    Append  $Q_i$  to  $\mathbf{Q}$ 
    Append first column of  $R_i$  to  $\mathbf{b}^{\text{red}}$                             // reduced bias for layer  $i$ 
    Append remainder of  $R_i$  to  $\mathbf{W}^{\text{red}}$                             // reduced weights for layer  $i$ 
    Set  $A_{i+1} \leftarrow [b_{i+1} \quad W_{i+1} Q_i \text{Inc}_i]$            // matrix of size  $n_{i+1} \times (n_i^{\text{red}} + 1)$ 
end
Append the first column of  $A_L$  to  $\mathbf{b}^{\text{red}}$                             // reduced bias for last layer
Append the remainder of  $A_L$  to  $\mathbf{W}^{\text{red}}$                             // reduced weights for last layer

return  $\mathbf{Q}, \mathbf{W}^{\text{red}}, \mathbf{b}^{\text{red}}$ 
  
```

---

230 We explain the notation of the algorithm. The inclusion matrix  $\text{Inc}_i \in \mathbb{R}^{n_i \times n_i^{\text{red}}}$  has  
 231 ones along the main diagonal and zeros elsewhere. The method QR-decomp with mode =  
 232 ‘complete’ computes the complete QR decomposition of the  $n_i \times (1 + n_{i-1}^{\text{red}})$  matrix  $A_i$   
 233 as  $Q_i \text{Inc}_i R_i$  where  $Q_i \in O(n_i)$  and  $R_i$  is upper-triangular of size  $n_i^{\text{red}} \times (1 + n_{i-1}^{\text{red}})$ . The  
 234 definition of  $n_i^{\text{red}}$  implies that either  $n_i^{\text{red}} = n_{i-1}^{\text{red}} + 1$  or  $n_i^{\text{red}} = n_i$ . The matrix  $R_i$  is of size  
 235  $n_i^{\text{red}} \times n_i^{\text{red}}$  in the former case and of size  $n_i \times (1 + n_{i-1}^{\text{red}})$  in the latter case.

236 **Example 6.** Suppose the widths of a radial neural network are  $(1, 8, 16, 8, 1)$ . Then it has  
 237  $\sum_{i=1}^4 (n_{i-1} + 1)n_i = 305$  trainable parameters. The reduced network has widths  $(1, 2, 3, 4, 1)$   
 238 and  $\sum_{i=1}^4 (n_{i-1}^{\text{red}} + 1)(n_i^{\text{red}}) = 34$  trainable parameters. Another example appears in Figure 4.

239 We note that the tuple of matrices  $\mathbf{Q}$  produced by Algorithm 1 does not feature in the  
 240 statement of Theorem 5, but is important in the proof (which appears in Appendix C).

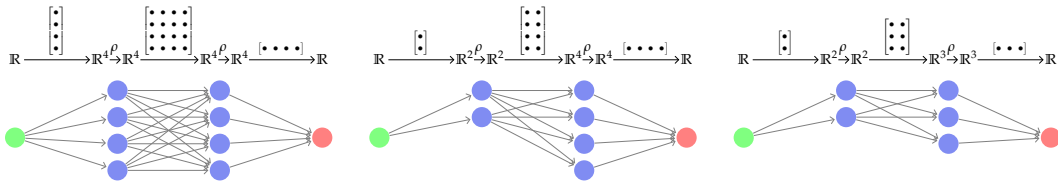


Figure 4: Model compression in 3 steps. Layer widths can be iteratively reduced to 1 greater than the previous. The number of trainable parameters reduces from 33 to 17.

241 Namely, an induction argument shows that the  $i$ -th partial feedforward function of the  
 242 original and reduced models are related via the matrices  $Q_i$  and  $\text{Inc}_i$ . A crucial ingredient  
 243 in the proof is that radial rescaling activations commute with orthogonal transformations.

## 244 6 Projected gradient descent

245 The typical use case for model compression algorithms is to produce a smaller version  
 246 of the fully trained model which can be deployed to make inference more efficient. It  
 247 is also worth considering whether compression can be used to accelerate training. For  
 248 example, for some compression algorithms, the compressed and full models have the same  
 249 feedforward function after a step of gradient descent is applied to each, and so one can  
 250 compress before training and still reach the same minimum. Unfortunately, in the context  
 251 of radial neural networks, compression using Algorithm 1 and then training does not  
 252 necessarily give the same result as training and then compression (see Appendix D.6 for a  
 253 counterexample). However, QR-compress does lead to a precise mathematical relationship  
 254 between optimization of the two models: the loss of the compressed model after one step  
 255 of gradient descent is equivalent to the loss of (a transformed version of) the original model  
 256 after one step of projected gradient descent. Proofs appear in Appendix D.

257 To state our results, fix a tuple of widths  $\mathbf{n}$  and a tuple  $\rho = (\rho_i : \mathbb{R}^{n_i} \rightarrow \mathbb{R}^{n_i})_{i=1}^L$  of radial  
 258 rescaling functions. The loss function  $\mathcal{L} : \text{Param}(\mathbf{n}) \rightarrow \mathbb{R}$  associated to a batch of training  
 259 data  $\{(x_j, y_j)\} \subseteq \mathbb{R}^{n_0} \times \mathbb{R}^{n_L}$  is defined as taking parameter values  $(\mathbf{W}, \mathbf{b})$  to the sum  
 260  $\sum_j \mathcal{C}(F(x_j), y_j)$  where  $\mathcal{C} : \mathbb{R}^{n_L} \times \mathbb{R}^{n_L} \rightarrow \mathbb{R}$  is a cost function on the output space, and  
 261  $F = F_{(\mathbf{W}, \mathbf{b}, \rho)}$  is the feedforward of the radial neural network with parameters  $(\mathbf{W}, \mathbf{b})$  and  
 262 activations  $\rho$ . Similarly, we have a loss function  $\mathcal{L}_{\text{red}}$  on the parameter space  $\text{Param}(\mathbf{n}^{\text{red}})$   
 263 with reduced widths vector. For any learning rate  $\eta > 0$ , we obtain gradient descent maps:

$$\begin{aligned} \gamma : \text{Param}(\mathbf{n}) &\rightarrow \text{Param}(\mathbf{n}) & \gamma_{\text{red}} : \text{Param}(\mathbf{n}^{\text{red}}) &\rightarrow \text{Param}(\mathbf{n}^{\text{red}}) \\ (\mathbf{W}, \mathbf{b}) &\mapsto (\mathbf{W}, \mathbf{b}) - \eta \nabla_{(\mathbf{W}, \mathbf{b})} \mathcal{L} & (\mathbf{V}, \mathbf{c}) &\mapsto (\mathbf{V}, \mathbf{c}) - \eta \nabla_{(\mathbf{V}, \mathbf{c})} \mathcal{L}_{\text{red}} \end{aligned}$$

264 We will also consider, for  $k \geq 0$ , the  $k$ -fold composition  $\gamma^k = \gamma \circ \gamma \circ \dots \circ \gamma$  and similarly  
 265 for  $\gamma_{\text{red}}$ . The *projected gradient descent* map on  $\text{Param}(\mathbf{n})$  is given by:

$$\gamma_{\text{proj}} : \text{Param}(\mathbf{n}) \rightarrow \text{Param}(\mathbf{n}), \quad (\mathbf{W}, \mathbf{b}) \mapsto \text{Proj}(\gamma(\mathbf{W}, \mathbf{b}))$$

266 where the map Proj zeroes out all entries in the bottom left  $(n_i - n_i^{\text{red}}) \times n_{i-1}^{\text{red}}$  submatrix of  
 267  $W_i - \nabla_{W_i} \mathcal{L}$ , and the bottom  $(n_i - n_i^{\text{red}})$  entries in  $b_i - \nabla_{b_i} \mathcal{L}$ , for each  $i$ . Schematically:

$$W_i - \nabla_{W_i} \mathcal{L} = \begin{bmatrix} * & * \\ * & * \end{bmatrix} \mapsto \begin{bmatrix} * & * \\ 0 & * \end{bmatrix}, \quad b_i - \nabla_{b_i} \mathcal{L} = \begin{bmatrix} * \\ * \end{bmatrix} \mapsto \begin{bmatrix} * \\ 0 \end{bmatrix}$$

268 To state the following theorem, let  $\mathbf{W}^{\text{red}}, \mathbf{b}^{\text{red}}, \mathbf{Q} = \text{QR-compress}(\mathbf{W}, \mathbf{b})$  be the outputs  
 269 of Algorithm 1 applied to  $(\mathbf{W}, \mathbf{b}) \in \text{Param}(\mathbf{n})$ . Hence  $(\mathbf{W}^{\text{red}}, \mathbf{b}^{\text{red}}) \in \text{Param}(\mathbf{n}^{\text{red}})$  are  
 270 the parameters of the compressed model, and  $\mathbf{Q} \in O(\mathbf{n}^{\text{hid}})$  is an orthogonal parameter  
 271 symmetry. We also consider the action (Section 5.1) of  $\mathbf{Q}^{-1}$  applied to  $(\mathbf{W}, \mathbf{b})$ .

272 **Theorem 7.** Let  $\mathbf{W}^{\text{red}}, \mathbf{b}^{\text{red}}, \mathbf{Q} = \text{QR-compress}(\mathbf{W}, \mathbf{b})$  be the outputs of Algorithm 1 applied to  
 273  $(\mathbf{W}, \mathbf{b}) \in \text{Param}(\mathbf{n})$ . Set  $\mathbf{U} = \mathbf{Q}^{-1} \cdot (\mathbf{W}, \mathbf{b}) - (\mathbf{W}^{\text{red}}, \mathbf{b}^{\text{red}})$ . For any  $k \geq 0$ , we have:

$$\gamma^k(\mathbf{W}, \mathbf{b}) = \mathbf{Q} \cdot \gamma^k(\mathbf{Q}^{-1} \cdot (\mathbf{W}, \mathbf{b})) \quad \gamma_{\text{proj}}^k(\mathbf{Q}^{-1} \cdot (\mathbf{W}, \mathbf{b})) = \gamma_{\text{red}}^k(\mathbf{W}^{\text{red}}, \mathbf{b}^{\text{red}}) + \mathbf{U}.$$

274 We conclude that gradient descent with initial values  $(\mathbf{W}, \mathbf{b})$  is equivalent to gradient  
 275 descent with initial values  $\mathbf{Q}^{-1} \cdot (\mathbf{W}, \mathbf{b})$  since at any stage we can apply  $\mathbf{Q}^{\pm 1}$  to move from  
 276 one to the other. Furthermore, projected gradient descent with initial values  $\mathbf{Q}^{-1} \cdot (\mathbf{W}, \mathbf{b})$   
 277 is equivalent to gradient descent on  $\text{Param}(\mathbf{n}^{\text{red}})$  with initial values  $(\mathbf{W}^{\text{red}}, \mathbf{b}^{\text{red}})$  since at  
 278 any stage we can move from one to the other by  $\pm \mathbf{U}$ . **Neither  $\mathbf{Q}$  nor  $\mathbf{U}$  depends on  $k$ .**



## 7 Experiments

In addition to the theoretical results in this work, we provide an implementation of Algorithm 1, in order to validate the claims of Theorems 5 and 7 empirically, as well as to quantify real-world performance. Full experimental details are in Appendix E.

**(1) Empirical verification of Theorem 5.** We learn the function  $f(x) = e^{-x^2}$  from samples using a radial neural network with widths  $\mathbf{n} = (1, 6, 7, 1)$  and activation the radial shifted sigmoid  $h(x) = 1/(1 + e^{-x+s})$ . Applying QR-compress gives a compressed radial neural network with widths  $\mathbf{n}^{\text{red}} = (1, 2, 3, 1)$ . Theorem 5 implies that the respective neural functions  $F$  and  $F_{\text{red}}$  are equal. Over 10 random initializations, the mean absolute error is negligible up to machine precision:  $(1/N) \sum_j |F(x_j) - F_{\text{red}}(x_j)| = 1.31 \cdot 10^{-8} \pm 4.45 \cdot 10^{-9}$ .

**(2) Empirical verification of Theorem 7.** The claim is that training the transformed model with parameters  $\mathbf{Q}^{-1} \cdot (\mathbf{W}, \mathbf{b})$  and objective  $\mathcal{L}$  by projected gradient descent coincides with training the reduced model with parameters  $(\mathbf{W}^{\text{red}}, \mathbf{b}^{\text{red}})$  and objective  $\mathcal{L}_{\text{red}}$  by usual gradient descent. We verified this on synthetic data as above. Over 10 random initializations, the loss functions after training match:  $|\mathcal{L} - \mathcal{L}_{\text{red}}| = 4.02 \cdot 10^{-9} \pm 7.01 \cdot 10^{-9}$ .

**(3) The compressed model trains faster.** Our compression method may be applied before training to produce a smaller model class which *trains* faster without sacrificing accuracy. We demonstrate this in learning the function  $f : \mathbb{R}^2 \rightarrow \mathbb{R}^2$  sending  $(t_1, t_2)$  to  $(e^{-t_1^2}, e^{-t_2^2})$  using a radial neural network with widths  $\mathbf{n} = (2, 16, 64, 128, 16, 2)$  and activation the radial sigmoid  $h(r) = 1/(1 + e^{-r})$ . Applying QR-compress gives a compressed network with widths  $\mathbf{n}^{\text{red}} = (2, 3, 4, 5, 6, 2)$ . We trained both models until the training loss was  $\leq 0.01$ . Over 10 random initializations on our system, the reduced network trained in  $15.32 \pm 2.53$  seconds and the original network trained in  $31.24 \pm 4.55$  seconds.

## 8 Conclusions and Discussion

This paper demonstrates that radial neural networks are universal approximators and that their parameter spaces exhibit a rich symmetry group, leading to a model compression algorithm. The results of this work combine to build a theoretical foundation for the use of radial neural networks, and suggest that radial neural networks hold promise for wider practical applicability. Furthermore, this work makes an argument for considering the advantages of non-pointwise nonlinearities in neural networks.

There are two main limitations of our results, each providing an opportunity for future work. First, our universal approximation constructions currently work only for Step-ReLU radial rescaling radial activations; it would be desirable to generalize to other activations. Additionally, Theorem 5 achieves compression only for networks whose widths satisfy  $n_i > n_{i-1} + 1$  for some  $i$ . Neural networks which do not have increasing widths anywhere in their architecture, such as encoders, would not be compressible.

Further extensions of this work include: First, little is currently known about the stability properties of radial neural networks during training, as well as their sensitivity to initialization. Second, radial rescaling activations provide an extreme case of symmetry; there may be benefits to combining radial and pointwise activations within a single network, for example, through ‘block’ radial rescaling functions. Third, the parameter space symmetries may provide a key ingredient in analyzing the gradient flow dynamics of radial neural networks and computation of conserved quantities. Fourth, radial rescaling activations can be used within convolutional or group-equivariant NNs. Finally, based on the theoretical advantages laid out in this paper, future work will explore empirically applications in which we expect radial networks to outperform alternate methods. Such potential applications include data spaces with circular or distance-based class boundaries.

## References

- [1] Lei Jimmy Ba and Rich Caruana. Do deep nets really need to be deep? *arXiv:1312.6184*, 2013. 3
- [2] Erkao Bao and Linqi Song. Equivariant neural networks and equivarification. *arXiv:1906.07172*, 2019. 3
- [3] Davis Blalock, Jose Javier Gonzalez Ortiz, Jonathan Frankle, and John Gutttag. What is the state of neural network pruning? *arXiv:2003.03033*, 2020. 3
- [4] David S Broomhead and David Lowe. Radial basis functions, multi-variable functional interpolation and adaptive networks. Technical report, Royal Signals and Radar Establishment Malvern (United Kingdom), 1988. 1, 3
- [5] Cristian Buciluă, Rich Caruana, and Alexandru Niculescu-Mizil. Model compression. In *Proceedings of the 12th ACM SIGKDD International Conference on Knowledge Discovery and Data Mining*, pages 535–541, 2006. 3
- [6] Yu Cheng, X Yu Felix, Rogerio S Feris, Sanjiv Kumar, Alok Choudhary, and Shih-Fu Chang. Fast neural networks with circulant projections. *arXiv:1502.03436*, 2, 2015. 3
- [7] Yu Cheng, Felix X Yu, Rogerio S Feris, Sanjiv Kumar, Alok Choudhary, and Shi-Fu Chang. An exploration of parameter redundancy in deep networks with circulant projections. In *Proceedings of the IEEE international conference on computer vision*, pages 2857–2865, 2015. 3
- [8] Yu Cheng, Duo Wang, Pan Zhou, and Tao Zhang. A survey of model compression and acceleration for deep neural networks. *arXiv:1710.09282*, 2017. 3
- [9] Benjamin Chidester, Minh N. Do, and Jian Ma. Rotation equivariance and invariance in convolutional neural networks. *arXiv:1805.12301*, 2018. 3
- [10] Djork-Arné Clevert, Thomas Unterthiner, and Sepp Hochreiter. Fast and accurate deep network learning by exponential linear units (elus). *arXiv preprint arXiv:1511.07289*, 2015. 1
- [11] Taco S. Cohen and Max Welling. Group equivariant convolutional networks. In *International conference on machine learning (ICML)*, pages 2990–2999, 2016. 3
- [12] Taco S Cohen and Max Welling. Steerable CNNs. In *Proceedings of the International Conference on Learning Representations (ICLR)*, 2017. 3
- [13] Taco S. Cohen, Maurice Weiler, Berkay Kicanaoglu, and Max Welling. Gauge equivariant convolutional networks and the icosahedral CNN. In *Proceedings of the 36th International Conference on Machine Learning (ICML)*, volume 97, pages 1321–1330, 2019. 3
- [14] George Cybenko. Approximation by superpositions of a sigmoidal function. *Mathematics of control, signals and systems*, 2(4):303–314, 1989. 1, 3
- [15] Congyue Deng, O. Litany, Yueqi Duan, A. Poulenard, A. Tagliasacchi, and L. Guibas. Vector Neurons: A General Framework for SO(3)-Equivariant Networks. *2021 IEEE/CVF International Conference on Computer Vision (ICCV)*, 2021. doi: 10.1109/iccv48922.2021.01198. 3
- [16] Sander Dieleman, Jeffrey De Fauw, and Koray Kavukcuoglu. Exploiting cyclic symmetry in convolutional neural networks. In *International Conference on Machine Learning (ICML)*, 2016. 3
- [17] Xin Dong, Shangyu Chen, and Sinno Jialin Pan. Learning to prune deep neural networks via layer-wise optimal brain surgeon. *arXiv preprint arXiv:1705.07565*, 2017. 3

- [18] Jonathan Frankle and Michael Carbin. The lottery ticket hypothesis: Finding sparse, trainable neural networks. *arXiv:1803.03635*, 2018. 3
- [19] Yunchao Gong, Liu Liu, Ming Yang, and Lubomir Bourdev. Compressing deep convolutional networks using vector quantization. *arXiv:1412.6115*, 2014. 3
- [20] Song Han, Huizi Mao, and William J Dally. Deep compression: Compressing deep neural networks with pruning, trained quantization and Huffman coding. *arXiv:1510.00149*, 2015. 3
- [21] Charles R. Harris, K. Jarrod Millman, Stéfan J. van der Walt, Ralf Gommers, Pauli Virtanen, David Cournapeau, Eric Wieser, Julian Taylor, Sebastian Berg, Nathaniel J. Smith, Robert Kern, Matti Picus, Stephan Hoyer, Marten H. van Kerkwijk, Matthew Brett, Allan Haldane, Jaime Fernández del Río, Mark Wiebe, Pearu Peterson, Pierre Gérard-Marchant, Kevin Sheppard, Tyler Reddy, Warren Weckesser, Hameer Abbasi, Christoph Gohlke, and Travis E. Oliphant. Array programming with NumPy. *Nature*, 585(7825):357–362, September 2020. doi: 10.1038/s41586-020-2649-2. URL <https://doi.org/10.1038/s41586-020-2649-2>. 34
- [22] Babak Hassibi and David G Stork. *Second order derivatives for network pruning: Optimal brain surgeon*. Morgan Kaufmann, 1993. 3
- [23] Geoffrey Hinton, Oriol Vinyals, and Jeff Dean. Distilling the knowledge in a neural network. *arXiv:1503.02531*, 2015. 3
- [24] Kurt Hornik. Approximation capabilities of multilayer feedforward networks. *Neural networks*, 4(2):251–257, 1991. 3
- [25] Andrew G Howard, Menglong Zhu, Bo Chen, Dmitry Kalenichenko, Weijun Wang, Tobias Weyand, Marco Andreetto, and Hartwig Adam. Mobilenets: Efficient convolutional neural networks for mobile vision applications. *arXiv:1704.04861*, 2017. 3
- [26] George Jeffreys and Siu-Cheong Lau. Kähler Geometry of Quiver Varieties and Machine Learning. *arXiv:2101.11487*, 2021. URL <http://arxiv.org/abs/2101.11487>. 3
- [27] Ehud D Karnin. A simple procedure for pruning back-propagation trained neural networks. *IEEE transactions on neural networks*, 1(2):239–242, 1990. 3
- [28] Patrick Kidger and Terry Lyons. Universal approximation with deep narrow networks. In *Conference on learning theory*, pages 2306–2327. PMLR, 2020. 3
- [29] Günter Klambauer, Thomas Unterthiner, Andreas Mayr, and Sepp Hochreiter. Self-normalizing neural networks. *Advances in neural information processing systems*, 30, 2017. 1
- [30] Risi Kondor and Shubhendu Trivedi. On the Generalization of Equivariance and Convolution in Neural Networks to the Action of Compact Groups. In *International conference on machine learning (ICML)*, 2018. 3
- [31] Leon Lang and Maurice Weiler. A Wigner-Eckart theorem for group equivariant convolution kernels. In *International Conference on Learning Representations (ICLR)*, 2021. 3
- [32] Vadim Lebedev, Yaroslav Ganin, Maksim Rakhuba, Ivan Oseledets, and Victor Lempitsky. Speeding-up convolutional neural networks using fine-tuned cp-decomposition. *arXiv:1412.6553*, 2014. 3
- [33] Yann LeCun, John S Denker, and Sara A Solla. Optimal brain damage. In *Advances in neural information processing systems*, pages 598–605, 1990. 3

- [34] Namhoon Lee, Thalaiyasingam Ajanthan, Stephen Gould, and Philip HS Torr. A signal propagation perspective for pruning neural networks at initialization. *arXiv preprint arXiv:1906.06307*, 2019. 3
- [35] Yongxi Lu, Abhishek Kumar, Shuangfei Zhai, Yu Cheng, Tara Javidi, and Rogerio Feris. Fully-adaptive feature sharing in multi-task networks with applications in person attribute classification. In *Proceedings of the IEEE conference on computer vision and pattern recognition (CVPR)*, pages 5334–5343, 2017. 3
- [36] Zhou Lu, Hongming Pu, Feicheng Wang, Zhiqiang Hu, and Liwei Wang. The expressive power of neural networks: A view from the width. *Advances in neural information processing systems*, 30, 2017. 3
- [37] Mirco Millettari, Thiparat Chotibut, and Paolo E Trevisanutto. Mean field theory of activation functions in deep neural networks. *arXiv preprint arXiv:1805.08786*, 2018. 1
- [38] Diganta Misra. Mish: A self regularized non-monotonic activation function. *arXiv preprint arXiv:1908.08681*, 2019. 1
- [39] Pavlo Molchanov, Stephen Tyree, Tero Karras, Timo Aila, and Jan Kautz. Pruning convolutional neural networks for resource efficient inference. *arXiv preprint arXiv:1611.06440*, 2016. 3
- [40] Jooyoung Park and Irwin W Sandberg. Universal approximation using radial-basis-function networks. *Neural computation*, 3(2):246–257, 1991. 3
- [41] Adam Paszke, Sam Gross, Francisco Massa, Adam Lerer, James Bradbury, Gregory Chanan, Trevor Killeen, Zeming Lin, Natalia Gimelshein, Luca Antiga, Alban Desmaison, Andreas Kopf, Edward Yang, Zachary DeVito, Martin Raison, Alykhan Tejani, Sasank Chilamkurthy, Benoit Steiner, Lu Fang, Junjie Bai, and Soumith Chintala. Pytorch: An imperative style, high-performance deep learning library. In H. Wallach, H. Larochelle, A. Beygelzimer, F. d Alché-Buc, E. Fox, and R. Garnett, editors, *Advances in Neural Information Processing Systems (NeurIPS)* 32, pages 8024–8035. Curran Associates, Inc., 2019. URL <http://papers.neurips.cc/paper/9015-pytorch-an-imperative-style-high-performance-deep-learning-library.pdf>. 34
- [42] Prajit Ramachandran, Barret Zoph, and Quoc V Le. Searching for activation functions. *arXiv preprint arXiv:1710.05941*, 2017. 1
- [43] Siamak Ravanbakhsh. Universal equivariant multilayer perceptrons. In *International Conference on Machine Learning*, pages 7996–8006. PMLR, 2020. 3
- [44] Siamak Ravanbakhsh, Jeff Schneider, and Barnabas Poczos. Equivariance through parameter-sharing. In *International Conference on Machine Learning*, pages 2892–2901. PMLR, 2017. 3
- [45] Roberto Rigamonti, Amos Sironi, Vincent Lepetit, and Pascal Fua. Learning separable filters. In *Proceedings of the IEEE conference on computer vision and pattern recognition*, pages 2754–2761, 2013. 3
- [46] Frank Rosenblatt. The perceptron: a probabilistic model for information storage and organization in the brain. *Psychological review*, 65(6):386, 1958. 1
- [47] Sara Sabour, Nicholas Frosst, and Geoffrey E Hinton. Dynamic routing between capsules. *arXiv:1710.09829*, 2017. 2, 3
- [48] Thiago Serra, Abhinav Kumar, and Srikumar Ramalingam. Lossless compression of deep neural networks. In *International Conference on Integration of Constraint Programming, Artificial Intelligence, and Operations Research*, pages 417–430. Springer, 2020. 3

- [49] Thiago Serra, Xin Yu, Abhinav Kumar, and Srikumar Ramalingam. Scaling up exact neural network compression by relu stability. *Advances in Neural Information Processing Systems*, 34, 2021. 3
- [50] Sho Sonoda and Noboru Murata. Neural network with unbounded activation functions is universal approximator. *Applied and Computational Harmonic Analysis*, 43(2): 233–268, 2017. 3
- [51] Gustav Sourek, Filip Zelezny, and Ondrej Kuzelka. Lossless compression of structured convolutional models via lifting. *arXiv preprint arXiv:2007.06567*, 2020. 3
- [52] Cheng Tai, Tong Xiao, Yi Zhang, Xiaogang Wang, et al. Convolutional neural networks with low-rank regularization. *arXiv:1511.06067*, 2015. 3
- [53] Chaoqi Wang, Guodong Zhang, and Roger Grosse. Picking winning tickets before training by preserving gradient flow. *arXiv preprint arXiv:2002.07376*, 2020. 3
- [54] Ming-Xi Wang and Yang Qu. Approximation capabilities of neural networks on unbounded domains. *Neural Networks*, 145:56–67, 2022. 3
- [55] Maurice Weiler and Gabriele Cesa. General  $E(2)$ -Equivariant Steerable CNNs. *Conference on Neural Information Processing Systems (NeurIPS)*, 2019. 2, 3, 4
- [56] Maurice Weiler, Mario Geiger, Max Welling, Wouter Boomsma, and Taco Cohen. 3D steerable CNNs: Learning rotationally equivariant features in volumetric data. *Proceedings of the 32nd International Conference on Neural Information Processing Systems (NeurIPS)*, 2018. 2, 3
- [57] Maurice Weiler, Fred A Hamprecht, and Martin Storath. Learning steerable filters for rotation equivariant CNNs. In *Proceedings of the IEEE Conference on Computer Vision and Pattern Recognition (CVPR)*, pages 849–858, 2018. 2, 3
- [58] Daniel E Worrall, Stephan J Garbin, Daniyar Turmukhambetov, and Gabriel J Brostow. Harmonic networks: Deep translation and rotation equivariance. In *Proceedings of the IEEE Conference on Computer Vision and Pattern Recognition (CVPR)*, pages 5028–5037, 2017. 3
- [59] Jiaxiang Wu, Cong Leng, Yuhang Wang, Qinghao Hu, and Jian Cheng. Quantized convolutional neural networks for mobile devices. In *Proceedings of the IEEE Conference on Computer Vision and Pattern Recognition (CVPR)*, pages 4820–4828, 2016. 3
- [60] Dmitry Yarotsky. Universal approximations of invariant maps by neural networks. *Constructive Approximation*, 55(1):407–474, 2022. 3
- [61] Tianyun Zhang, Shaokai Ye, Kaiqi Zhang, Jian Tang, Wujie Wen, Makan Fardad, and Yanzhi Wang. A systematic DNN weight pruning framework using alternating direction method of multipliers. In *Proceedings of the European Conference on Computer Vision (ECCV)*, pages 184–199, 2018. 3

## Checklist

### 1. For all authors...

- (a) Do the main claims made in the abstract and introduction accurately reflect the paper's contributions and scope? [\[Yes\]](#)
- (b) Did you describe the limitations of your work? [\[Yes\]](#) See Section 8.
- (c) Did you discuss any potential negative societal impacts of your work? [\[N/A\]](#)  
Our work is theoretical and does not hold specific risks of negative impacts.
- (d) Have you read the ethics review guidelines and ensured that your paper conforms to them? [\[Yes\]](#)

### 2. If you are including theoretical results...

- (a) Did you state the full set of assumptions of all theoretical results? [\[Yes\]](#)
- (b) Did you include complete proofs of all theoretical results? [\[Yes\]](#) Most of the proofs appear in the supplementary material.

### 3. If you ran experiments...

- (a) Did you include the code, data, and instructions needed to reproduce the main experimental results (either in the supplemental material or as a URL)? [\[Yes\]](#)
- (b) Did you specify all the training details (e.g., data splits, hyperparameters, how they were chosen)? [\[Yes\]](#)
- (c) Did you report error bars (e.g., with respect to the random seed after running experiments multiple times)? [\[Yes\]](#)
- (d) Did you include the total amount of compute and the type of resources used (e.g., type of GPUs, internal cluster, or cloud provider)? [\[Yes\]](#) See Appendix E.

### 4. If you are using existing assets (e.g., code, data, models) or curating/releasing new assets...

- (a) If your work uses existing assets, did you cite the creators? [\[Yes\]](#)
- (b) Did you mention the license of the assets? [\[N/A\]](#)
- (c) Did you include any new assets either in the supplemental material or as a URL? [\[N/A\]](#)
- (d) Did you discuss whether and how consent was obtained from people whose data you're using/curating? [\[N/A\]](#)
- (e) Did you discuss whether the data you are using/curating contains personally identifiable information or offensive content? [\[N/A\]](#)

### 5. If you used crowdsourcing or conducted research with human subjects...

- (a) Did you include the full text of instructions given to participants and screenshots, if applicable? [\[N/A\]](#)
- (b) Did you describe any potential participant risks, with links to Institutional Review Board (IRB) approvals, if applicable? [\[N/A\]](#)
- (c) Did you include the estimated hourly wage paid to participants and the total amount spent on participant compensation? [\[N/A\]](#)